

Search for the Blazhko effect in field RR Lyrae stars using LINEAR and ZTF light curves

Ema Donev¹ and Željko Ivezić²

¹ XV. Gymnasium (MIOC), Jordanovac 8, 10000, Zagreb, Croatia, e-mail: emadonev@icloud.com

² Department of Astronomy and the DiRAC Institute, University of Washington, 3910 15th Avenue NE, Seattle, WA, USA e-mail: ivezic@uw.edu

October 2024

ABSTRACT

We analyzed the incidence and properties of RR Lyrae stars that show evidence for amplitude and phase modulation (the so-called Blazhko Effect) in a sample of $\sim 3,000$ stars with LINEAR and ZTF light curve data collected during the periods of 2002–2008 and 2018–2023, respectively. A preliminary subsample of about ~ 500 stars was algorithmically pre-selected using various data quality and light curve statistics, and then 228 stars were confirmed visually as displaying the Blazhko effect. This sample nearly doubles the number of field RR Lyrae stars displaying the Blazhko effect and places a lower limit of $(11.4 \pm 0.8)\%$ for their incidence rate. We find that ab type RR Lyrae that show the Blazhko effect have about 5% (0.030 day) shorter periods than starting sample, a 7.1σ statistically significant difference. We find no significant differences in their light curve amplitudes and apparent magnitude (essentially, signal-to-noise ratio) distributions. No period or other differences are found for c type RR Lyrae. We find convincing examples of stars where the Blazhko effect can appear and disappear on time scales of several years. With time-resolved photometry expected from LSST, a similar analysis will be performed for even larger samples of fields RR Lyrae stars in the southern sky and we anticipate a higher fraction of discovered Blazhko stars due to better sampling and superior photometric quality.

Key words. Variable stars — RR Lyrae stars — Blazhko Effect

1. Introduction

RR Lyrae stars are pulsating variable stars with periods in the range of 3–30 hours and large amplitudes that increase towards blue optical bands (e.g., in the SDSS g band from 0.2 mag to 1.5 mag; Sesar et al. 2010). For comprehensive reviews of RR Lyrae stars, we refer the reader to Smith (1995) and Catelan (2009).

RR Lyrae stars often exhibit amplitude and phase modulation, or the so-called Blazhko effect¹ (hereafter, “Blazhko stars”). For examples of well-sampled observed light curves showing the Blazhko effect, see, e.g., Kepler data shown in Figures 1 and 2 from Benkő et al. (2010). The Blazhko effect has been known for a long time (Blažko 1907), but its detailed observational properties and theoretical explanation of its causes remain elusive (Kolenberg 2008; Kovács 2009; Szabó 2014). Various proposed models for the Blazhko effect, and principal reasons why they fail to explain observations, are summarized in Kovacs (2016).

A part of the reason for the incomplete observational description of the Blazhko effect is difficulties in discovering a large number of Blazhko stars due to temporal baselines that are too short and insufficient number of observations per object (Kovacs 2016; Hernitschek & Stassun 2022). With the advent of modern sky surveys, several studies reported large increases in the number of known Blazhko stars, starting with a sample of about 700 Blazhko stars discovered by the MACHO survey towards the LMC (Alcock et al. 2003) and about 500 Blazhko stars discovered by the OGLE-II survey towards the Galactic bulge (Miz-

erski 2003). Most recently, about 4,000 Blazhko stars were discovered in the LMC and SMC (Soszyński et al. 2009, 2010), and an additional $\sim 3,500$ stars were discovered in the Galactic bulge (Soszyński et al. 2011; Prudil & Skarka 2017), both by the OGLE-III survey. Nevertheless, discovering the Blazhko effect in field RR Lyrae stars that are spread over the entire sky remains a much harder problem: only about 200 Blazhko stars in total from all the studies of field RR Lyrae stars have been reported so far (see Table 1 in Kovacs 2016).

Here, we report the results of a search for the Blazhko effect in a sample of $\sim 3,000$ field RR Lyrae stars with LINEAR and ZTF light curve data. A preliminary subsample of about ~ 500 stars was selected using various light curve statistics, and then 228 stars were confirmed visually as displaying the Blazhko effect. This new sample doubles the number of field RR Lyrae stars that exhibit the Blazhko effect. In §2 and §3 we describe our datasets and analysis methodology, and in §4 we present our analysis results. Our main results are summarized and discussed in §5.

2. Data Description and Period Estimation

Analysis of field RR Lyrae stars requires a sensitive time-domain photometric survey over a large sky area. For our starting sample, we used $\sim 3,000$ field RR Lyrae stars with light curves obtained by the LINEAR asteroid survey. In order to study long-term changes in light curves, we also utilized light curves obtained by the ZTF survey which monitored the sky ~ 15 years after LINEAR. The combination of LINEAR and ZTF provided

¹ The Blazhko effect was discovered by Lidiya Petrovna Tseraskaya and first reported by Sergey Blazhko.

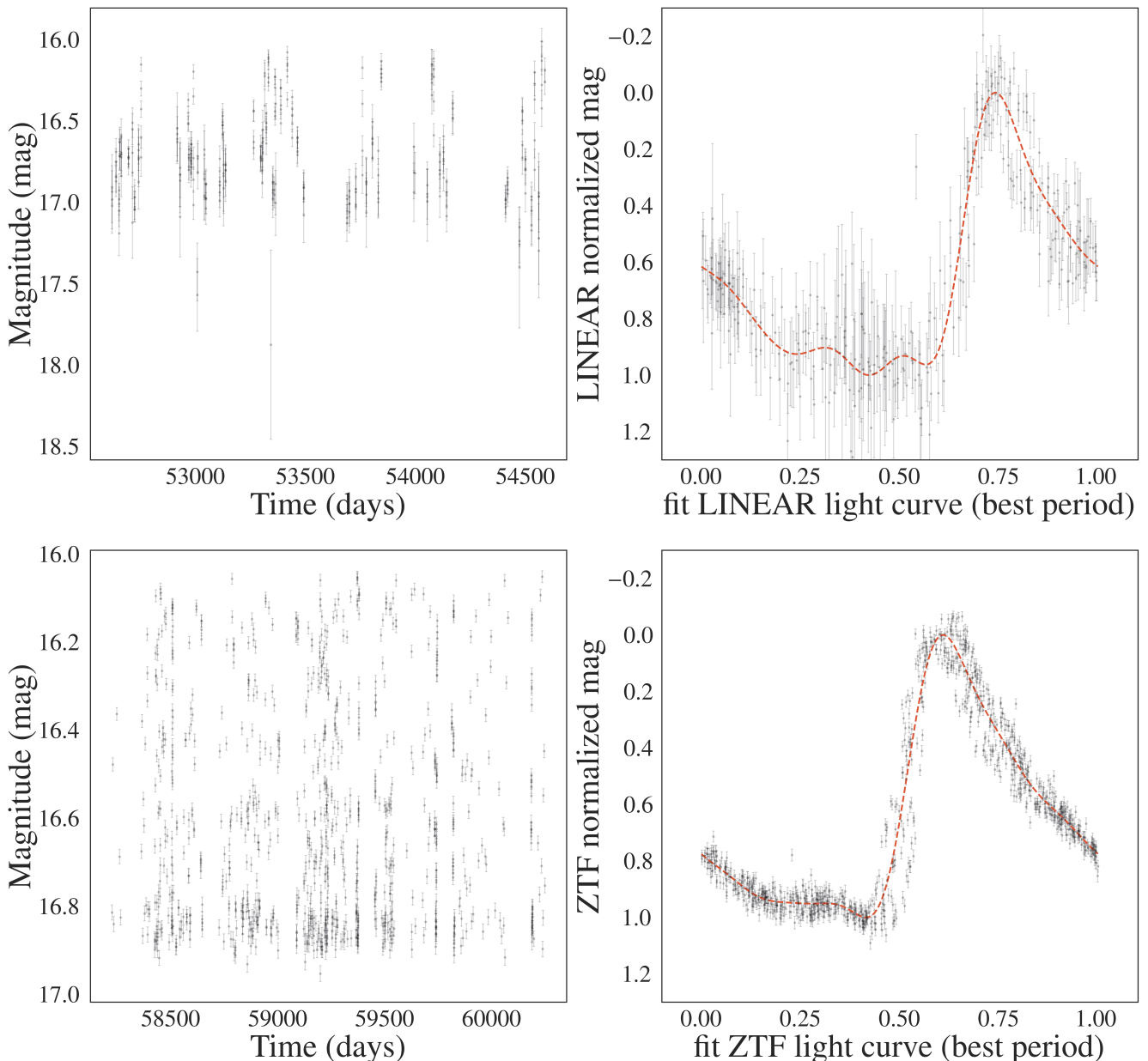


Fig. 1. An example of a Blazhko star (LINEARid = 136668) with LINEAR (top row) and ZTF (bottom row) light curves (left panels, data points with “error bars”), phased light curves normalized to the 0–1 range (right panels, data points with “error bars”), with their best-fit models shown by dashed lines. The best-fit period is determined for each dataset separately using 3 Fourier terms. The models shown in the right panels are evaluated with 6 Fourier terms.

56 a unique opportunity to systematically search for the Blazhko effect
 57 in a large number of field RR Lyrae stars over a large time
 58 span of two decades.

59 We first describe each dataset in more detail, and then introduce our analysis methods. All our analysis code, written in
 60 Python, is available on GitHub².

62 2.1. LINEAR Dataset

63 The properties of the LINEAR asteroid survey and its photometric
 64 re-calibration based on SDSS data are discussed in Sesar et al.
 65 (2011). Briefly, the LINEAR survey covered about 10,000 deg²
 66 of the northern sky in white light (no filters were used, see Fig. 1
 67 in Sesar et al. 2011), with photometric errors ranging from ~0.03

68 mag at an equivalent SDSS magnitude of $r = 15$ to 0.20 mag at
 69 $r \sim 18$. Light curves used in this work include, on average, 270
 70 data points collected between December 2002 and September
 71 2008.

72 A sample of 7,010 periodic variable stars with $r < 17$ discovered
 73 in LINEAR data were robustly classified by Palaversa et al.
 74 (2013), including about ~3,000 field RR Lyrae stars of both ab
 75 and c type, detected to distances of about 30 kpc (Sesar et al.
 76 2013). The sample used in this work contains 2196 ab-type and
 77 745 c-type RR Lyrae, selected using classification labels and the
 78 gi color index from Palaversa et al. (2013). The LINEAR light
 79 curves, augmented with IDs, equatorial coordinates, and other
 80 data, were accessed using the astroML Python module³ (VanderPlas
 81 et al. 2012).

³ For an example of light curves, see https://www.astroml.org/book_figures/chapter10/fig_LINEAR_LS.html

² https://github.com/emadonev/var_stars

82 2.2. ZTF Dataset

83 The Zwicky Transient Factory (ZTF) is an optical time-domain
 84 survey that uses the Palomar 48-inch Schmidt telescope and a
 85 camera with 47 deg² field of view (Bellm et al. 2019). The
 86 dataset analyzed here was obtained with SDSS-like *g*, *r*, and *i*
 87 band filters. Light curves for objects in common with the LIN-
 88 EAR RR Lyrae sample typically have smaller random photomet-
 89 ric errors than LINEAR light curves because ZTF data are deeper
 90 (compared to LINEAR, ZTF data have about 2-3 magnitudes
 91 fainter 5 σ depth). ZTF data used in this work were collected
 92 between February 2018 and December 2023, on average about
 93 15 years after obtaining LINEAR data. The median number of
 94 observations per star for ZTF light curves is ~500.

95 The ZTF dataset for this project was created by selecting
 96 ZTF IDs with matching equatorial coordinates to a correspond-
 97 ing LINEAR ID of an RR Lyrae star. This process used the
 98 *ztfquery* function, which searched the coordinates in the ZTF
 99 database within 3 arcsec from the LINEAR position. The result-
 100 ing sample consisted of 2857 RR Lyrae stars with both LINEAR
 101 and ZTF data. The fractions of RRab and RRc type RR Lyrae in
 102 this sample, 71% RRab and 29% RRc type, are consistent with
 103 results from other surveys (e.g., Sesar et al. 2010).

104 2.3. Period Estimation

105 The first step of our analysis is estimating best-fit periods, sepa-
 106 rately for LINEAR and ZTF datasets. We used the Lomb-Scargle
 107 method (Vanderplas 2015) as implemented in *astropy* (Astropy
 108 Collaboration et al. 2018). The period estimation used 3 Fourier
 109 components and a two-step process: an initial best-fit frequency
 110 was determined using the *autopower* frequency grid option and
 111 then the power spectrum was recomputed around the initial fre-
 112 quency using an order of magnitude smaller frequency step. In
 113 case of ZTF, we estimated period separately for each available
 114 passband and adopted their median value. Once the best-fit pe-
 115 riod was determined, a best-fit model for the phased light curve
 116 was computed using 6 Fourier components. Fig 1 shows an ex-
 117 ample of a star with LINEAR and ZTF light curves, phased light
 118 curves, and their best-fit models.

119 We found excellent agreement between the best-fit periods
 120 estimated separately from LINEAR and ZTF light curves. The
 121 median of their ratio is unity within 2×10^{-6} and the robust stan-
 122 dard deviation of their ratio is 2×10^{-5} . With a median sample
 123 period of 0.56 days, the implied scatter of period difference is
 124 about 1.0 sec.

125 Given on average about 15 years between LINEAR and ZTF
 126 data sets, and a typical period of 0.56 days, this time difference
 127 corresponds to about 10,000 oscillations. With a fractional pe-
 128 riod uncertainty of 2×10^{-5} , LINEAR data can predict the phase
 129 of ZTF light curve with an uncertainty of 0.2. Therefore, for a
 130 robust detection of light curve phase modulation, each data set
 131 must be analyzed separately. On the other hand, amplitude mod-
 132 ulation can be detected on time scales as long as 15 years, as
 133 discussed in the following section.

134 3. Analysis Methodology: Searching for the Blazhko 135 Effect

136 Given the two sets of light curves from LINEAR and ZTF, we
 137 searched for amplitude and phase modulation, either during the
 138 5-6 years of data taking by each survey, or during the average
 139 span of 15 years between the two surveys. Starting with a sam-
 140 ple of 2857 RR Lyrae stars, we pre-selected a smaller sample

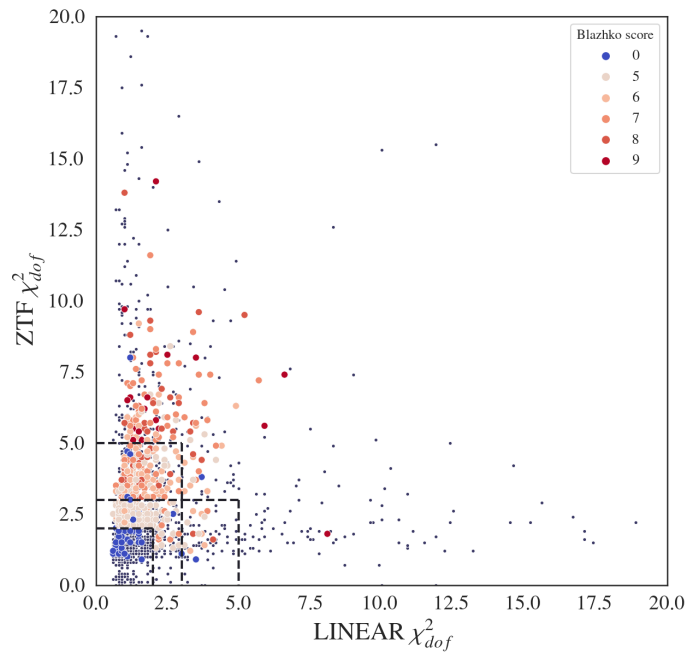


Fig. 2. A selection diagram constructed with the two sets of robust χ^2_{dof} values, for LINEAR and ZTF data sets, where the dark blue dots represent all RR Lyrae stars and the circles represent candidate Blazhko stars (color-coded according to the legend, with *B_score* representing the number of points scored from the selection algorithm). The horizontal and vertical dashed lines help visualize selection boundaries for Blazhko candidates (see text).

that was inspected visually (see below for details). We also re-
 141 quired at least 150 LINEAR data points and 150 ZTF data points
 142 (for the selected band from which we calculated the period) in
 143 analyzed light curves. We used two pre-selection methods that
 144 are sensitive to different types of light curve modulation: direct
 145 light curve analysis and periodogram analysis, as follows.
 146

3.1. Direct Light Curve Analysis

Given statistically correct period, amplitude and light curve
 148 shape estimates, as well as data being consistent with reported
 149 (presumably Gaussian) uncertainty estimates, the χ^2 per degree
 150 of freedom gives a quantitative assessment of the "goodness of
 151 fit",
 152

$$\chi^2_{dof} = \frac{1}{N_{dof}} \sum \frac{(d_i - m_i)^2}{\sigma_i^2}. \quad (1)$$

Here, d_i are measured light curve data values at times t_i , and
 153 with associated uncertainties σ_i , m_i are best-fit models at times
 154 t_i , and N_{dof} is the number of degrees of freedom, essentially the
 155 number of data points. In the absence of any light curve mod-
 156 ulation, the expected value of χ^2_{dof} is unity, with a standard devia-
 157 tion of $\sqrt{2/N_{dof}}$. If $\chi^2_{dof} - 1$ is many times larger than $\sqrt{2/N_{dof}}$,
 158 it is unlikely that data d_i were generated by the assumed (unchang-
 159 ing) model m_i . Of course, χ^2_{dof} can also be large due to
 160 underestimated measurement uncertainties σ_i , or to occasional
 161 non-Gaussian measurement error (the so-called outliers).

Therefore, to search for signatures of the Blazhko effect,
 163 manifested through statistically unlikely large values of χ^2_{dof} ,
 164 we computed χ^2_{dof} separately for LINEAR and ZTF data (see
 165 Fig. 2). Using the two sets of χ^2_{dof} values, we algorithmically pre-
 166

Analysis of blazhko star metrics for RR Lyrae

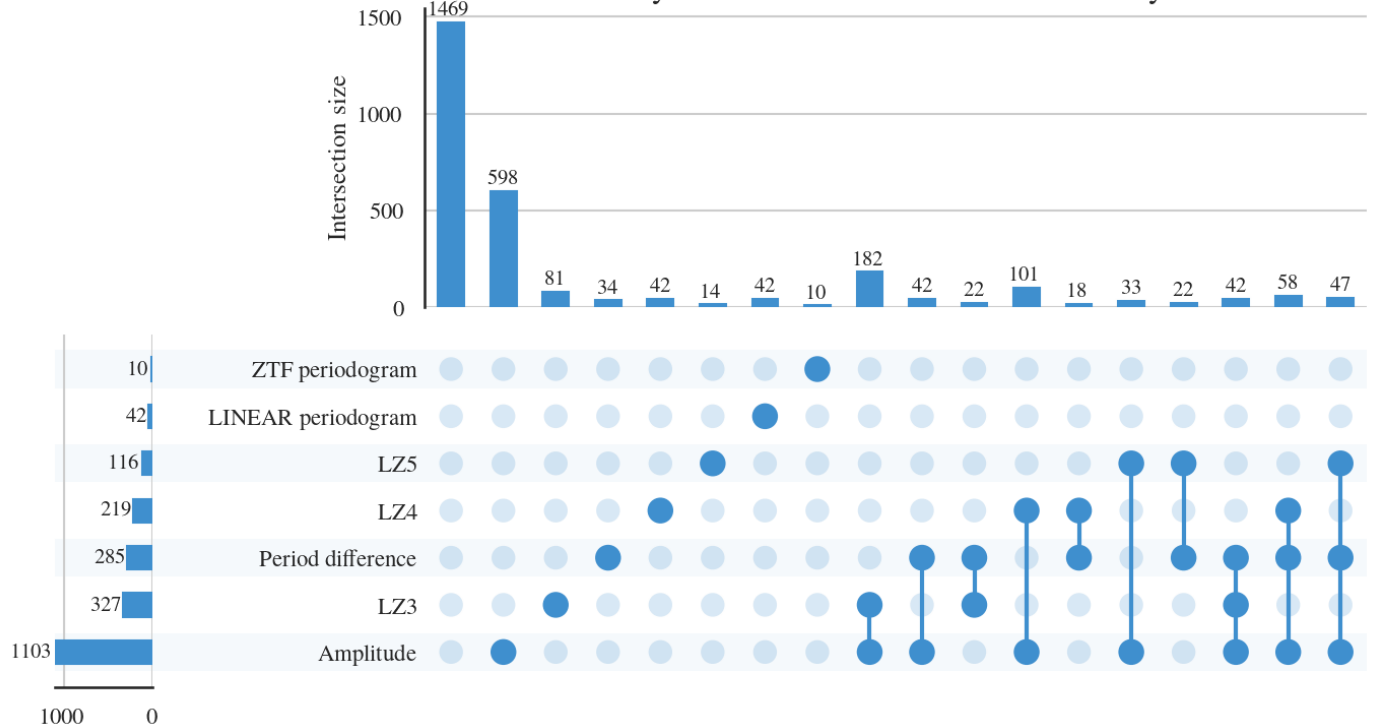


Fig. 3. The figure shows selection criteria and the resulting numbers of pre-selected Blazhko star candidates for each criterion and their combinations (x in LZx corresponds to the number of scored points in the χ^2_{dof} vs. χ^2_{dof} diagram (see Fig. 2). The dots represent each case a star can occupy, where every solid dot is a specific criterion that is satisfied. Connections between solid dots represent stars which satisfy multiple criteria. Each dot combination has its own count, represented by the horizontal countplot. The vertical countplot shows the total number of stars that satisfy one criteria (union of all cases). For example, a total of 116 stars passed the LZ5 criterion, with 14 of them satisfying only χ^2 criterion, 33 also had a significant amplitude change, 22 had a significant period difference, and 47 had both a significant period and amplitude difference along with the satisfied χ^2 criterion. The sum of all specific cases is 116.

selected a sample of candidate Blazhko stars for further visual analysis of their light curves. The visual analysis is needed to confirm the expected Blazhko behavior in observed light curves, as well as to identify cases of data problems, such as photometric outliers.

We used a simple scoring algorithm, optimized through trial and error, that utilized the two values of χ^2_{dof} , augmented by period and amplitude differences, as follows. A star could score a maximum of 9 points, and a minimum of 5 points was required for further visual analysis. The χ^2_{dof} selection boundaries are illustrated in Fig. 2. If either value of χ^2_{dof} exceeded 5, or both exceeded 3, a star was awarded 5 points and immediately selected for further analysis. If these χ^2_{dof} criteria were not met, a star could still be selected by meeting less stringent χ^2_{dof} selection if it also had large period or amplitude difference between LINEAR and ZTF datasets. Stars with at least one value of χ^2_{dof} above 2 would receive 3 points and those with at least one χ^2_{dof} above 3 would receive 4 points. A period difference exceeding 2×10^{-4} day would be awarded 1 point and two points for exceeding 5×10^{-4} day. Analogous limits for amplitude difference were 0.05 mag and 0.15 mag, respectively.

The candidate Blazhko sample pre-selected using this method includes 531 stars. For most selected stars, the χ^2_{dof} values were larger for the ZTF data because the ZTF photometric uncertainties are smaller than for the LINEAR data set. Fig. 3 summarizes the selection criteria and the resulting numbers of selected stars for each criterion and their combinations.

3.2. Periodogram Analysis

When light curve modulation is due to double-mode oscillation with two similar oscillation frequencies (periods), it is possible to recognize its signature in the periodogram computed as part of the Lomb-Scargle analysis. Depending on various details, such as data sampling and the exact values of periods, amplitudes, this method may be more efficient than direct light curve analysis (Skarka et al. 2020). We also employed this method to select additional candidates, as follows.

A sum of two *sine* functions with same amplitudes and with frequencies f_1 and f_2 can be rewritten using trigonometric equalities as

$$y(t) = 2 \cos\left(2\pi \frac{f_1 - f_2}{2} t\right) \sin\left(2\pi \frac{f_1 + f_2}{2} t\right). \quad (2)$$

We can define

$$f_o = \frac{f_1 + f_2}{2}, \quad (3)$$

and

$$\Delta f = \left| \frac{f_1 - f_2}{2} \right|, \quad (4)$$

with $\Delta f \ll f_o$ when f_1 and f_2 are similar. The fact that Δf is much smaller than f_o means that the period of the *cos* term is much larger than the period of the basic oscillation (f_o). In other words, the *cos* term acts as a slow amplitude modulation of the basic oscillation. When the amplitudes of two *sine* functions are

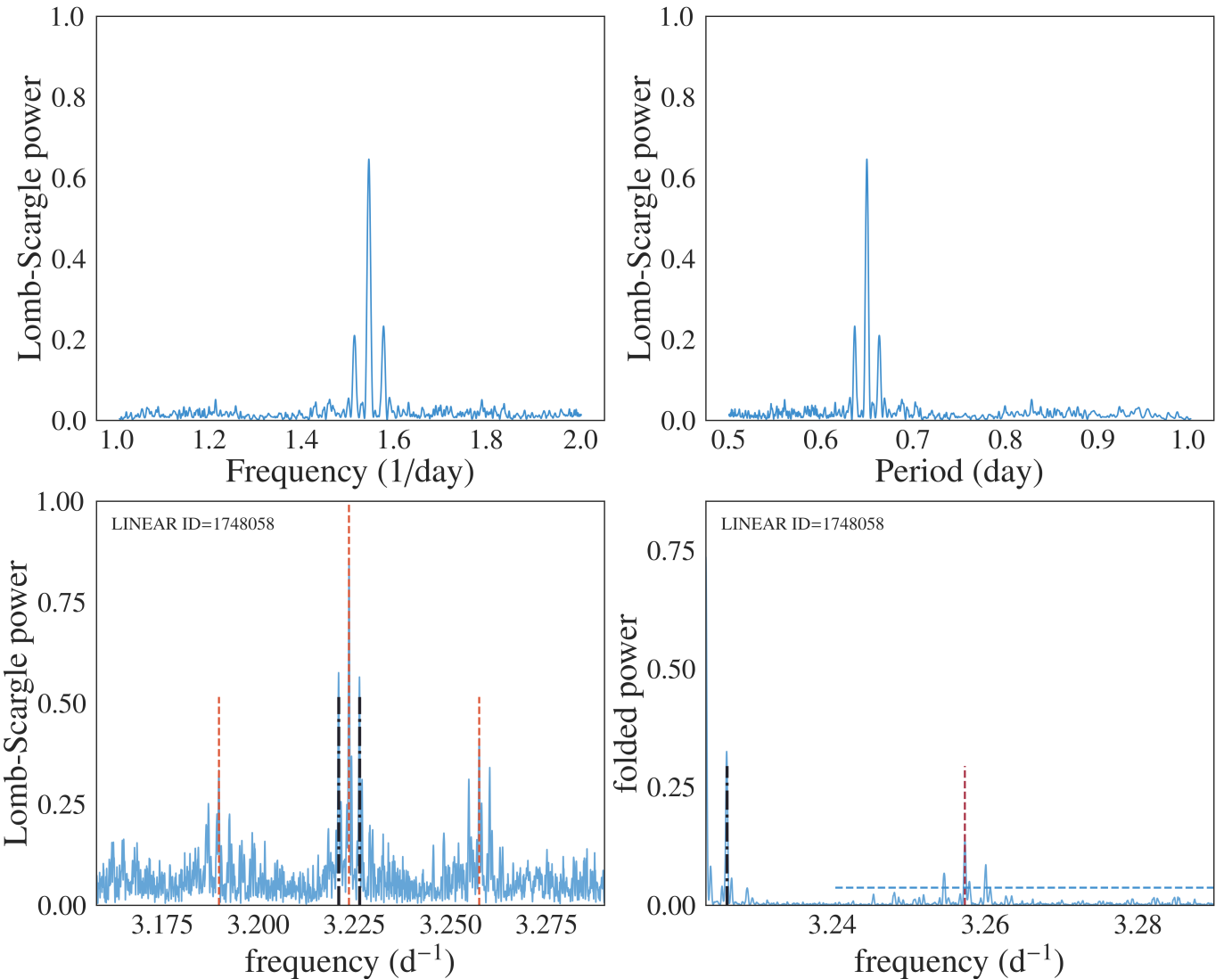


Fig. 4. The top two panels show a simulated periodogram for a sum of two *sine* functions with similar frequencies f_1 and f_2 – the central peak corresponds to their mean (see eqs. 3 and 4). The bottom left panel shows a periodogram for an observed LINEAR light curve for $ID = 1748058$, and the bottom right panel shows its folded version (around the main frequency $f_o = 3.223 \text{ d}^{-1}$). In the bottom left panel, the three vertical dashed lines show the three frequencies identified by the algorithm described in text, and the two dot-dashed lines mark yearly aliases around the main frequency f_o , at frequencies $f_o \pm 0.0274 \text{ d}^{-1}$. The two vertical lines in the bottom right panel have the same meaning, and the horizontal dashed line shows the noise level multiplied by 5.

not equal, the results are more complicated but the basic conclusion about amplitude modulation remains. When the power spectrum of $y(t)$ is constructed, it will show 3 peaks: the main peak at f_o and two more peaks at frequencies $f_o \pm \Delta f$. We used this fact to construct an algorithm for automated searching for the evidence of amplitude modulation. Fig 4 compares the theoretical periodogram produced by interference beats with our algorithm's periodogram, signifying that local Blazhko peaks are present in real data.

After the strongest peak in the Lomb-Scargle periodogram is found at frequency f_o , we search for two equally distant local peaks at frequencies f_- and f_+ , with $f_- < f_o < f_+$. The sideband peaks can be highly asymmetric Alcock et al. (2003) and observed periodograms can sometimes be much more complex Szczygieł & Fabrycky (2007). We fold the periodogram through the main peak at f_o , multiply the two branches and then search for the strongest peaks in the resulting folded periodogram that

is statistically more significant than the background noise. The background noise is computed as the scatter of the folded periodogram estimated from the interquartile range. We require a “signal-to-noise” ratio of at least 5, as well as the peak strength of at least 0.05 for ZTF, while 0.10 for LINEAR data. If such a peak is found, and it doesn't correspond to yearly alias, we select the star as a candidate Blazhko star and compute its Blazhko period as

$$P_{BL} = |f_{-,+} - f_0|^{-1},$$

where $f_{-,+}$ means the Blazhko sideband frequency with a higher amplitude is chosen.

The observed Blazhko periods range from 3 to 3,000 days, and Blazhko amplitudes range from 0.01 mag to about 0.3 mag (Szczygieł & Fabrycky 2007). In this work, we selected a smaller Blazhko range due to the limitations of our data: 30–325 days. With this additional constraint, we selected 52 candidate

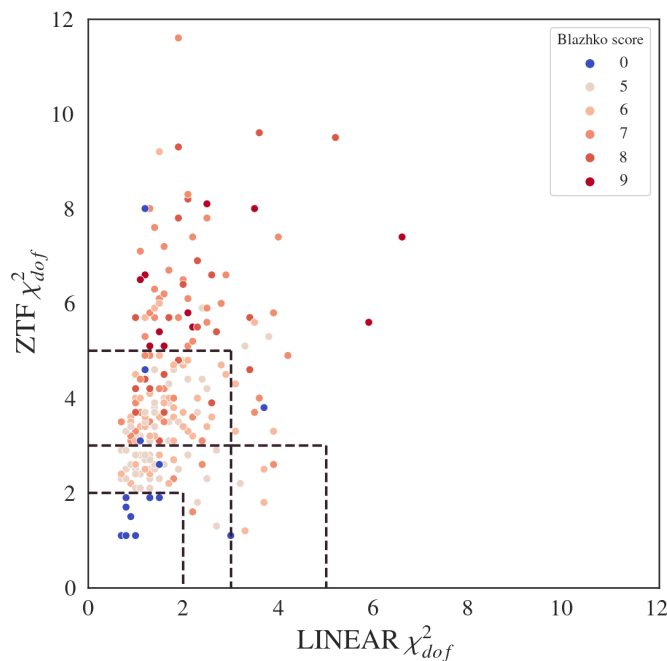


Fig. 5. Analogous to figure 2, except that here only 228 visually verified Blazhko stars are shown.

Blazhko stars. Fig. 4 shows an example where two very prominent peaks were identified in the LINEAR periodogram.

3.2.1. Visual Confirmation

The sample pre-selected for visual analysis includes 531 RR Lyrae stars (479 + 52), or 18.1% of the starting LINEAR-ZTF sample. Visual analysis included the following standard steps (e.g., Jurcsik et al. 2009; Prudil & Skarka 2017):

1. The shape of the phased light curves and scatter of data points around the best-fit model were examined for signatures of anomalous behavior indicative of the Blazhko effect. Fig. 6 shows an example of such behavior where the ZTF data and fit show multiple coherent data point sequences offset from the best-fit mean model.
2. Full light curves were inspected for their repeatability between observing seasons (Fig. 7). This step was sensitive to amplitude modulations with periods of the order a year or longer.
3. The phased light curves normalized to unit amplitude were inspected for their repeatability between observing seasons. This step was sensitive to phase modulations of a few percent or larger on time scales of the order a year or longer. Fig. 8 shows an example of a Blazhko star where season-to-season phase and amplitude modulations are seen in both the LINEAR data and (especially) the ZTF data. Another example is shown in Fig. 9 where only phase modulation is visible, without any discernible amplitude modulation.

After visually analyzing the starting sample of 531 Blazhko candidates, we visually confirmed expected Blazhko behavior for 228 stars (214 out of 479 and 14 out of 52). LINEAR IDs and other characteristics for confirmed Blazhko stars are listed in Table 1 (Appendix A). Statistical properties of the selected sample of Blazhko stars are discussed in detail in the next section.

4. Results

Starting with a sample of 2857 field RR Lyrae stars with both LINEAR and ZTF data, we constructed a subsample of 1996 with light curves of sufficient quality and selected and verified 228 stars that exhibit convincing Blazhko effect. In this section we compare various statistical properties of selected Blazhko stars to those of the starting sample.

4.1. The Blazhko Incidence Rate

The implied incidence rate for the Blazhko effect is $11.4 \pm 0.8\%$. Due to selection effects and unknown completeness, this rate should be considered as a lower limit. When ab and c types are considered separately, the rate is slightly higher for the former than for the latter: $12.1 \pm 0.9\%$ vs. $9.2 \pm 1.3\%$. The difference of 2.9% has low statistical significance ($< 2\sigma$).

4.2. Period, Amplitude and Magnitude Distributions

Marginal distributions of period, amplitude and apparent magnitude for the starting sample and Blazhko stars are compared in Fig. 10. Encouragingly, their magnitude distributions are statistically indistinguishable which indicates that the completeness is not a strong function of the photometric signal-to-noise ratio. This result is probably due to the fact that the sample is defined by the depth of LINEAR survey, while ZTF survey is deeper than this limit and its photometric quality is approximately constant across the probed magnitude range.

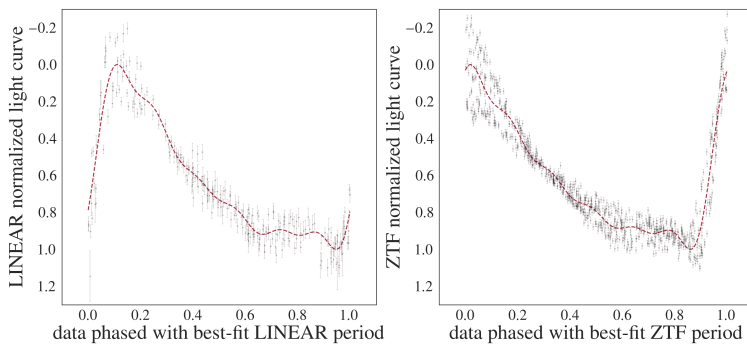
The suspected differences in amplitude and period distributions are further explored in Fig. 11. It is already discernible by eye that the period distribution for Blazhko stars of ab type is shifted to smaller values than for the starting sample. We have found that the median period for ab type Blazhko stars is about 5% shorter than for the starting RR Lyrae sample. This difference is significant at the 7.1σ level. At the same time, the difference in median amplitudes for ab type stars corresponds to only 0.6σ deviation. No statistically significant differences are found in period and amplitude distributions for c type stars.

If modulation amplitudes are correlated with periods such that larger modulation amplitudes occur in shorter period RRab stars, and if our selection efficiency is lower for smaller modulation amplitudes, then the detected period shift for ab type Blazhko stars might be at least partially due to combination of these two effects. This possibility does not appear likely. First, as we discussed in preceding section, our sample is defined by the depth of LINEAR survey, while ZTF survey is significantly deeper than this limit and its photometric quality is approximately constant across the probed magnitude range. Since it is sufficient for a star to display the Blazhko effect only in ZTF to be included in the sample, we do not expect strong selection effects (except for the LINEAR magnitude cutoff of course). Furthermore, Skarka et al. (2020) searched for period - modulation amplitude correlation using a large sample of stars with OGLE measurements and did not find any.

4.3. Long-term behavior of Blazhko Stars

During visual analysis, we noticed that some Blazhko stars exhibit convincing Blazhko effect either in LINEAR or in ZTF data, but not in both surveys. Fig. 12 shows an example where amplitude modulation is clearly seen in LINEAR light curves, while not discernible in ZTF light curves. There are also examples of stars where Blazhko effect is evident in ZTF but not in

STAR 160 from 239



LINEAR period chi robust: 2.1, LINEAR mean period chi robust: 2.1
ZTF period chi robust: 4.4, ZTF mean period chi robust: 4.4
LINEAR period chi: 8.7, LINEAR mean period chi: 8.7
ZTF period chi: 34.2, ZTF mean period chi: 34.2
LINEAR period: 0.545073, ZTF period: 0.545074, Period difference: 0.0
Average LINEAR magnitude: 15.25
LINEAR amplitude: 0.75, ZTF amplitude: 0.82

Fig. 6. An illustration of visual analysis of phased light curves for the selected Blazhko candidates. The left panel shows LINEAR data and the right panel shows ZTF data (symbols with “error bars”) for star with LINEARid = 10030349. The dashed lines are best-fit models. The numbers listed on the right side were added to aid visual analysis. Note multiple coherent data point sequences offset from the best-fit mean model in the right panel.

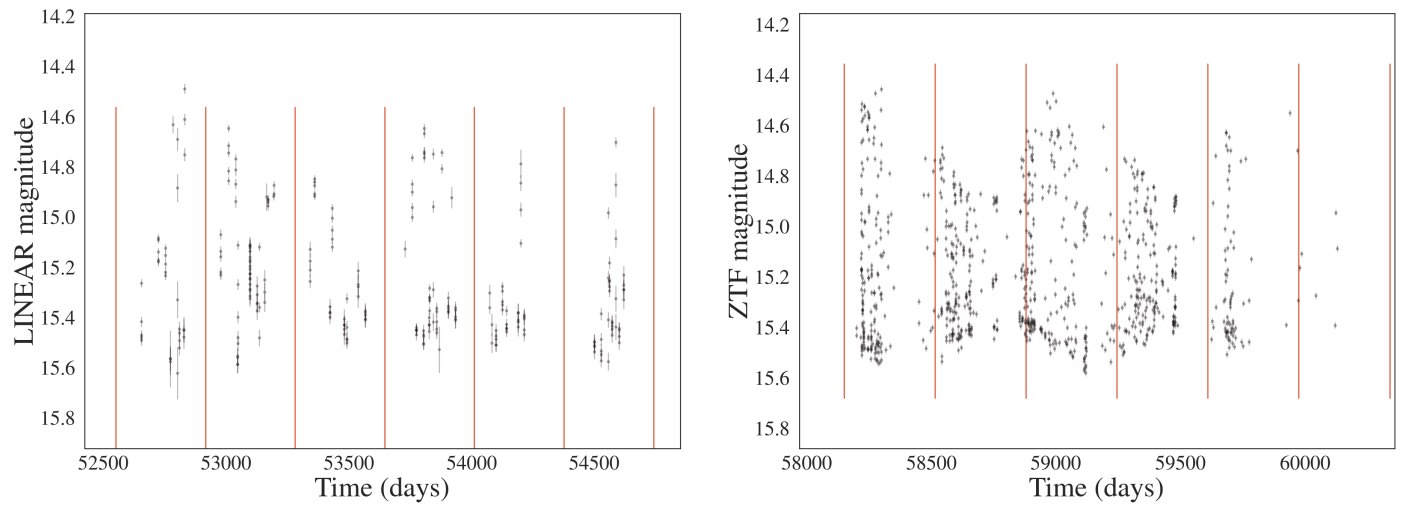


Fig. 7. An illustration of visual analysis of full light curves for the selected Blazhko candidates with emphasis on their repeatability between observing seasons, marked with vertical lines (left: LINEAR data; right: ZTF data). Data shown are for star with LINEARid = 10030349. Note strong amplitude modulation between observing seasons.

336 LINEAR data (e.g., LINEARid = 19466437, 14155360). This
337 finding strongly suggests that Blazhko effect can appear and dis-
338 appear on time scales shorter than about a decade.

339 5. Discussion and Conclusions

340 We found excellent agreement between the best-fit periods for
341 RR Lyrae stars estimated separately from LINEAR and ZTF
342 light curves. The sample of 228 stars presented here nearly dou-
343 bles the number of field RR Lyrae stars displaying the Blazhko
344 effect and places a lower limit of $(11.4 \pm 0.8)\%$ for their incidence
345 rate. The reported incidence rates for the Blazhko effect range
346 from 5% (Szczygieł & Fabrycky 2007) to 60% (Szabó et al.
347 2014). Differences in reported incidence rates can occur due to
348 varying data precision, the temporal baseline length, and differ-
349 ences in visual or algorithmic analysis. For a relatively small
350 sample of 151 stars with Kepler data, a claim has been made that
351 essentially every RR Lyrae star exhibits modulated light curve
352 (Kovacs 2018). The difference in Blazhko incidence rates for the
353 two most extensive samples, obtained by the OGLE-III survey
354 for the Large Magellanic Cloud (LMC, 20% out of 17,693 stars;
355 Soszyński et al. 2009) and the Galactic bulge (30% out of 11,756
356 stars; Soszyński et al. 2011) indicates a possible variation of the

Blazhko incidence rate with underlying stellar population prop-
357 erties.

We find that ab type RR Lyrae which show the Blazhko effect
358 have about 5% (0.030 day) shorter periods than starting sample.
359 While not large, the statistical significance of this difference is
360 7.1σ . At a similar uncertainty level ($\sim 1\%$), we don’t detect pe-
361 riod difference for c type stars, and don’t detect any difference
362 in amplitude distributions. We also find that for some stars the
363 Blazhko effect is discernible in only one dataset. This finding
364 strongly suggests that Blazhko effect can appear and disappear
365 on time scales shorter than about a decade, in agreement with
366 literature (Jurcsik et al. 2009; Poretti et al. 2010; Benkő et al.
367 2014).

The LINEAR and ZTF datasets analyzed in this work were
368 sufficiently large that we had to rely on algorithmic pruning of
369 the initial sample. The sample size problem will be even larger
370 for surveys such as the Legacy Survey of Space and Time (LSST;
371 Ivezić et al. 2019). LSST will be an excellent survey for study-
372 ing Blazhko effect (Hernitschek & Stassun 2022) because it will
373 have both a long temporal baseline (10 years) and a large number
374 of observations per object (nominally 825; LSST Science Re-
375 quirements Document⁴). We anticipate a higher fraction of dis-

⁴ Available as ls.st/srd

Seasons for:10030349

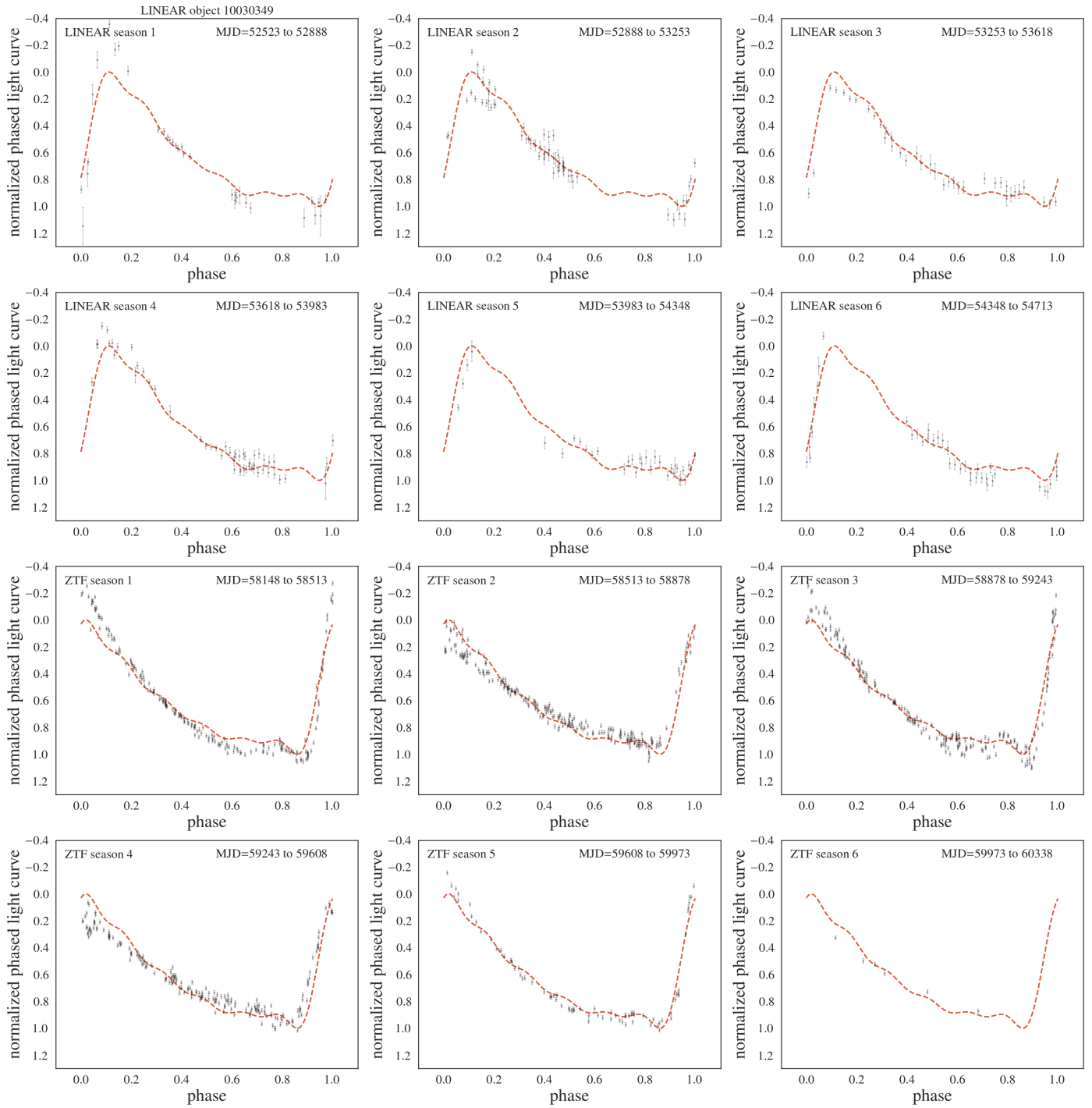


Fig. 8. The phased light curves normalized to unit amplitude of the overall best-fit model are shown for single observing seasons and compared to the mean best-fit models (top six panels: LINEAR data; bottom six panels: ZTF data). Data shown are for star with LINEARid = 10030349. Season-to-season phase and amplitude modulations are seen in both the LINEAR and the ZTF data.

379 covered Blazhko stars with LSST than reported here due to better
 380 sampling and superior photometric quality, since the incidence
 381 rate of the Blazhko effect increases with sensitivity to small-
 382 amplitude modulation, and thus with photometric data quality
 383 (Jurcsik et al. 2009).

384 The size and quality of LSST sample will motivate further
 385 developments of the selection algorithms. One obvious improve-
 386 ment will be inspection of neighboring objects to confirm pho-

387 tometric quality, as well as inspection of images to test implica-
 388 tion of an isolated point source (e.g., blended object photometry
 389 can be affected by variable seeing beyond aperture correction
 390 valid for isolated point sources). Another improvement is for-
 391 ward modeling of the Blazhko modulation, rather than searching
 392 for χ^2 outliers (Benkő et al. 2011; Guggenberger et al. 2012). For
 393 example, Skarka et al. (2020) classified Blazhko stars in 6 classes
 394 using the morphology of their amplitude modulation (the most

Seasons for: 16300450

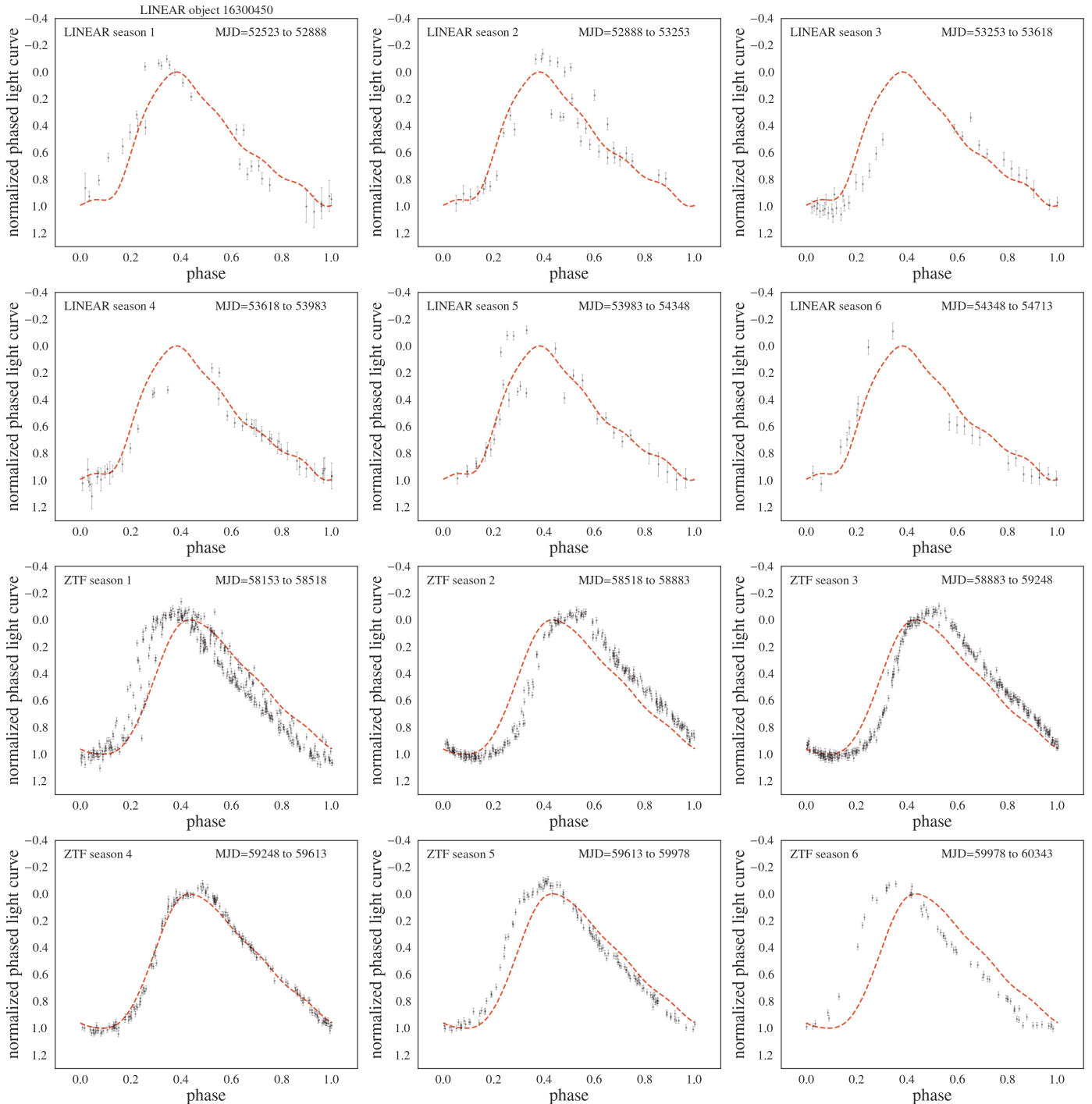


Fig. 9. Analogous to Fig. 8, except that star with LINEARid = 16300450 is shown. Unlike example shown in Fig. 8, only phase modulation is visible here, without any amplitude modulation, in both LINEAR and ZTF light curves.

dominant class includes 90% of the sample). They also found bimodal distribution of Blazhko periods, with two components centered on 48 d and 186 d. These results give hope that forward modeling of the Blazhko effect will improve the selection of such stars.

Acknowledgements. We thank Mathew Graham for providing *ztfquery* code example to us, and Robert Szabó for expert comments that improved presentation. Ž.I. acknowledges funding by the Fulbright Foundation and thanks the Ruđer Bošković Institute (Zagreb, Croatia) for hospitality. Based on observations ob-

tained with the Samuel Oschin Telescope 48-inch and the 60-inch Telescope at the Palomar Observatory as part of the Zwicky Transient Facility project. ZTF is supported by the National Science Foundation under Grants No. AST-1440341 and AST-2034437 and a collaboration including current partners Caltech, IPAC, the Weizmann Institute of Science, the Oskar Klein Center at Stockholm University, the University of Maryland, Deutsches Elektronen-Synchrotron and Humboldt University, the TANGO Consortium of Taiwan, the University of Wisconsin at Milwaukee, Trinity College Dublin, Lawrence Livermore National Laboratories, IN2P3, University of Warwick, Ruhr University Bochum, Northwestern University and former partners the University of Washington, Los Alamos National Laboratories, and Lawrence Berkeley National Laboratories. Operations

404
405
406
407
408
409
410
411
412
413
414

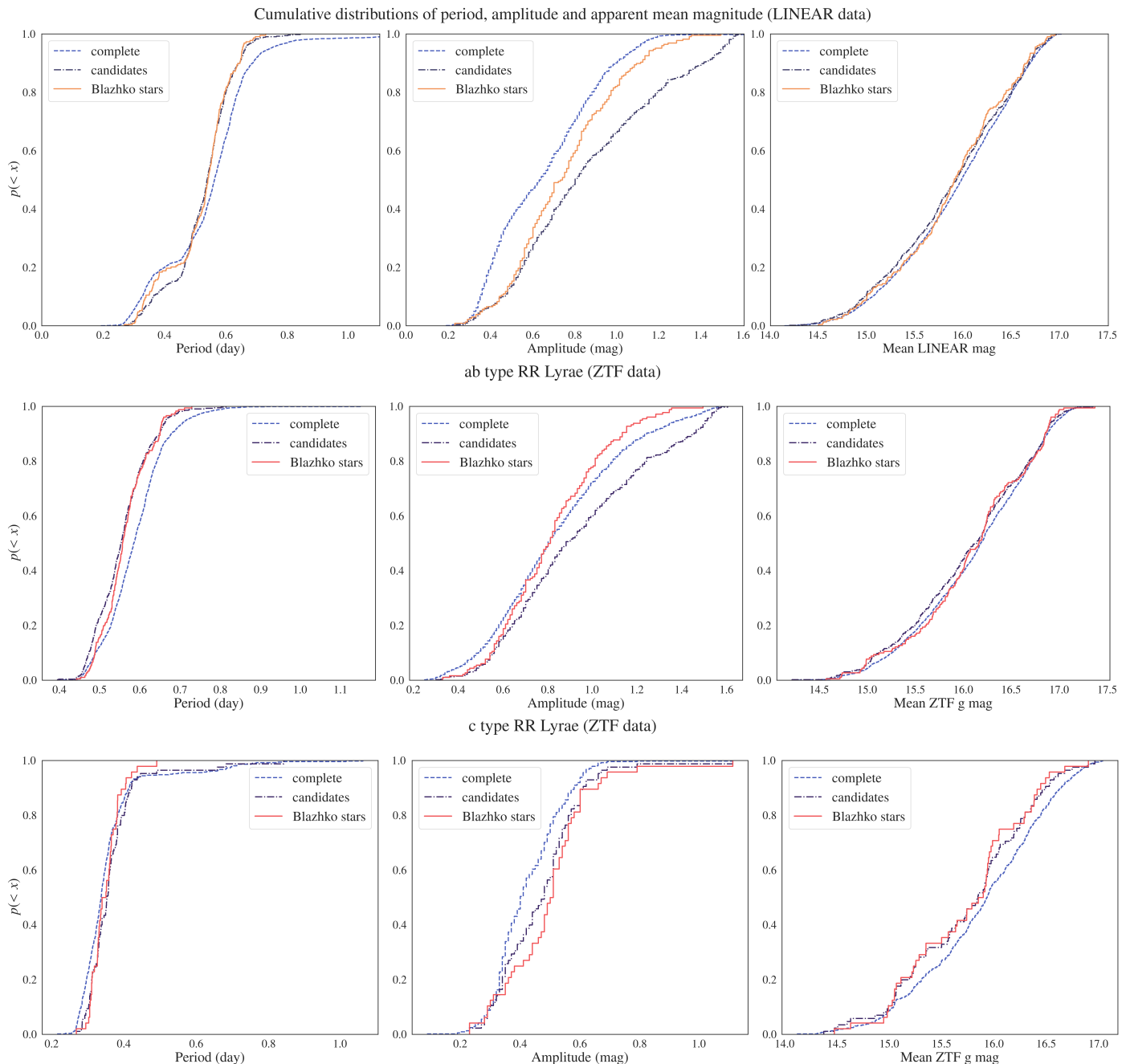


Fig. 10. A comparison of cumulative distributions of period (left), amplitude (middle) and apparent magnitude for starting sample, selected Blazhko candidates and visually verified Blazhko stars. The top row is based on LINEAR data and both ab type and c type stars. The middle and bottom rows are based on ZTF data, and show separately data for ab type and c type stars, respectively. The differences in period and amplitude distributions are further examined in figure 11.

415 are conducted by COO, IPAC, and UW. The LINEAR program is funded by
 416 the National Aeronautics and Space Administration at MIT Lincoln Laboratory
 417 under Air Force Contract FA8721-05-C-0002. Opinions, interpretations, conclusions
 418 and recommendations are those of the authors and are not necessarily endorsed by the United States Government.
 419

References

- | | |
|--|-----|
| Alcock, C., Alves, D. R., Becker, A., et al. 2003, ApJ, 598, 597 | 421 |
| Astropy Collaboration, Price-Whelan, A. M., Sipőcz, B. M., et al. 2018, AJ, 156, 123 | 422 |
| Bellm, E. C., Kulkarni, S. R., Graham, M. J., et al. 2019, PASP, 131, 018002 | 424 |
| Benkő, J. M., Kolenberg, K., Szabó, R., et al. 2010, MNRAS, 409, 1585 | 425 |
| Benkő, J. M., Plachy, E., Szabó, R., Molnár, L., & Kolláth, Z. 2014, ApJS, 213, 31 | 426 |
| Benkő, J. M., Szabó, R., & Paparó, M. 2011, MNRAS, 417, 974 | 427 |
| Blažko, S. 1907, Astronomische Nachrichten, 175, 325 | 428 |
| Catelan, M. 2009, Ap&SS, 320, 261 | 429 |
| Guggenberger, E., Kolenberg, K., Nemec, J. M., et al. 2012, MNRAS, 424, 649 | 430 |
| Hernitschek, N. & Stassun, K. G. 2022, ApJS, 258, 4 | 431 |
| Ivezić, Ž., Kahn, S. M., Tyson, J. A., et al. 2019, ApJ, 873, 111 | 432 |
| Jurcsik, J., Sódor, Á., Szeidl, B., et al. 2009, MNRAS, 400, 1006 | 433 |

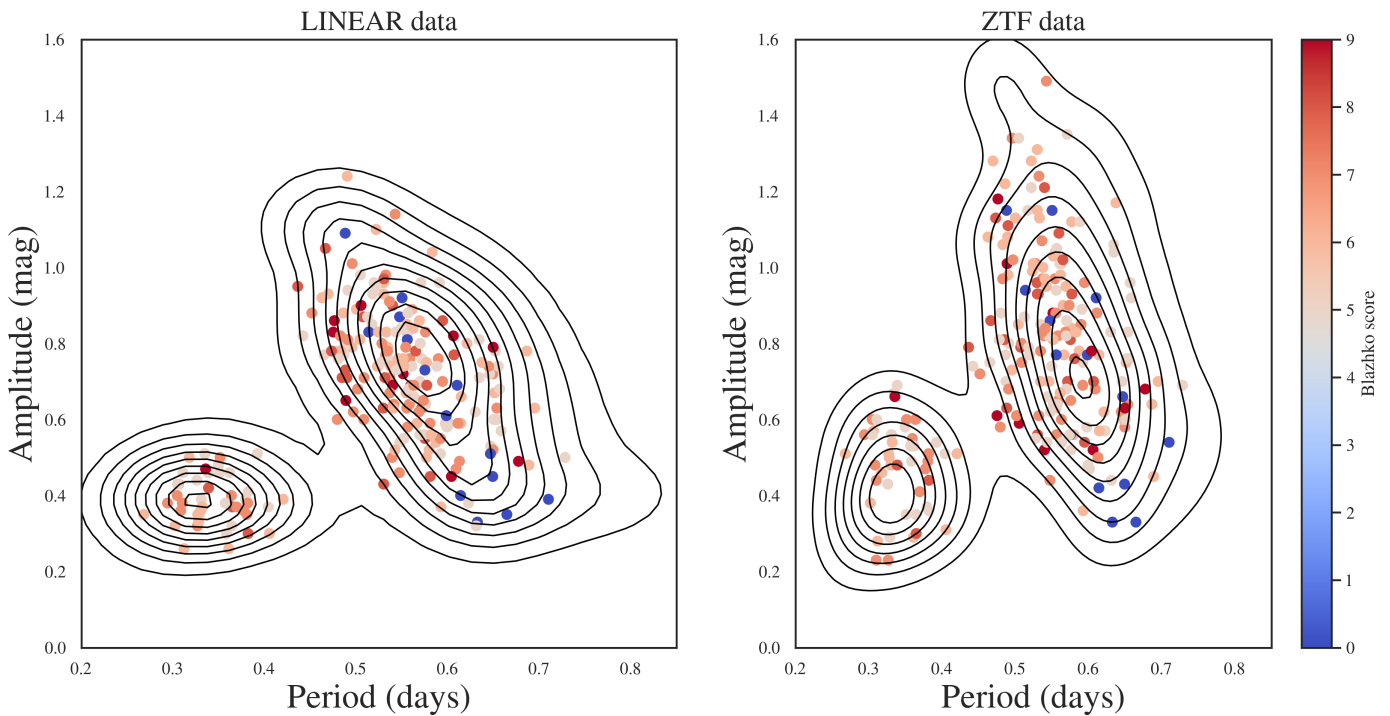


Fig. 11. Comparison of amplitude–period distributions (the Bailey diagram) for the starting sample of 1,996 RR Lyrae stars (contours) and 228 selected candidate Blazhko stars (symbols). The clump in the lower left corresponds to c type RR Lyrae and the other one to ab type. Note that the period distribution for ab type Blazhko stars is shifted left (by about 0.03 day, or 5%).

- 435 Kolenberg, K. 2008, in Journal of Physics Conference Series, Vol. 118, Journal
436 of Physics Conference Series (IOP), 012060
437 Kovács, G. 2009, in American Institute of Physics Conference Series, Vol. 1170,
438 Stellar Pulsation: Challenges for Theory and Observation, ed. J. A. Guzik &
439 P. A. Bradley, 261–272
440 Kovacs, G. 2016, Communications of the Konkoly Observatory Hungary, 105,
441 61
442 Kovacs, G. 2018, A&A, 614, L4
443 Mizerski, T. 2003, Acta Astron., 53, 307
444 Palaversa, L., Ivezić, Ž., Eyer, L., et al. 2013, AJ, 146, 101
445 Poretti, E., Paparó, M., Deleuil, M., et al. 2010, A&A, 520, A108
446 Prudil, Z. & Skarka, M. 2017, MNRAS, 466, 2602
447 Sesar, B., Ivezić, Ž., Grammer, S. H., et al. 2010, ApJ, 708, 717
448 Sesar, B., Ivezić, Ž., Stuart, J. S., et al. 2013, AJ, 146, 21
449 Sesar, B., Stuart, J. S., Ivezić, Ž., et al. 2011, AJ, 142, 190
450 Skarka, M., Prudil, Z., & Jurcsik, J. 2020, MNRAS, 494, 1237
451 Smith, H. A. 1995, Cambridge Astrophysics Series, 27
452 Soszyński, I., Dziembowski, W. A., Udalski, A., et al. 2011, Acta Astron., 61, 1
453 Soszyński, I., Udalski, A., Szymański, M. K., et al. 2010, Acta Astron., 60, 165
454 Soszyński, I., Udalski, A., Szymański, M. K., et al. 2009, Acta Astron., 59, 1
455 Szabó, R. 2014, in IAU Symposium, Vol. 301, Precision Asteroseismology, ed.
456 J. A. Guzik, W. J. Chaplin, G. Handler, & A. Pigulski, 241–248
457 Szabó, R., Benkő, J. M., Paparó, M., et al. 2014, A&A, 570, A100
458 Szczygieł, D. M. & Fabrycky, D. C. 2007, MNRAS, 377, 1263
459 Vanderplas, J. 2015, gatspy: General tools for Astronomical Time Series in
460 Python
461 VanderPlas, J., Connolly, A. J., Ivezić, Z., & Gray, A. 2012, in Proceedings of
462 Conference on Intelligent Data Understanding (CIDU), 47–54

Seasons for:3196780

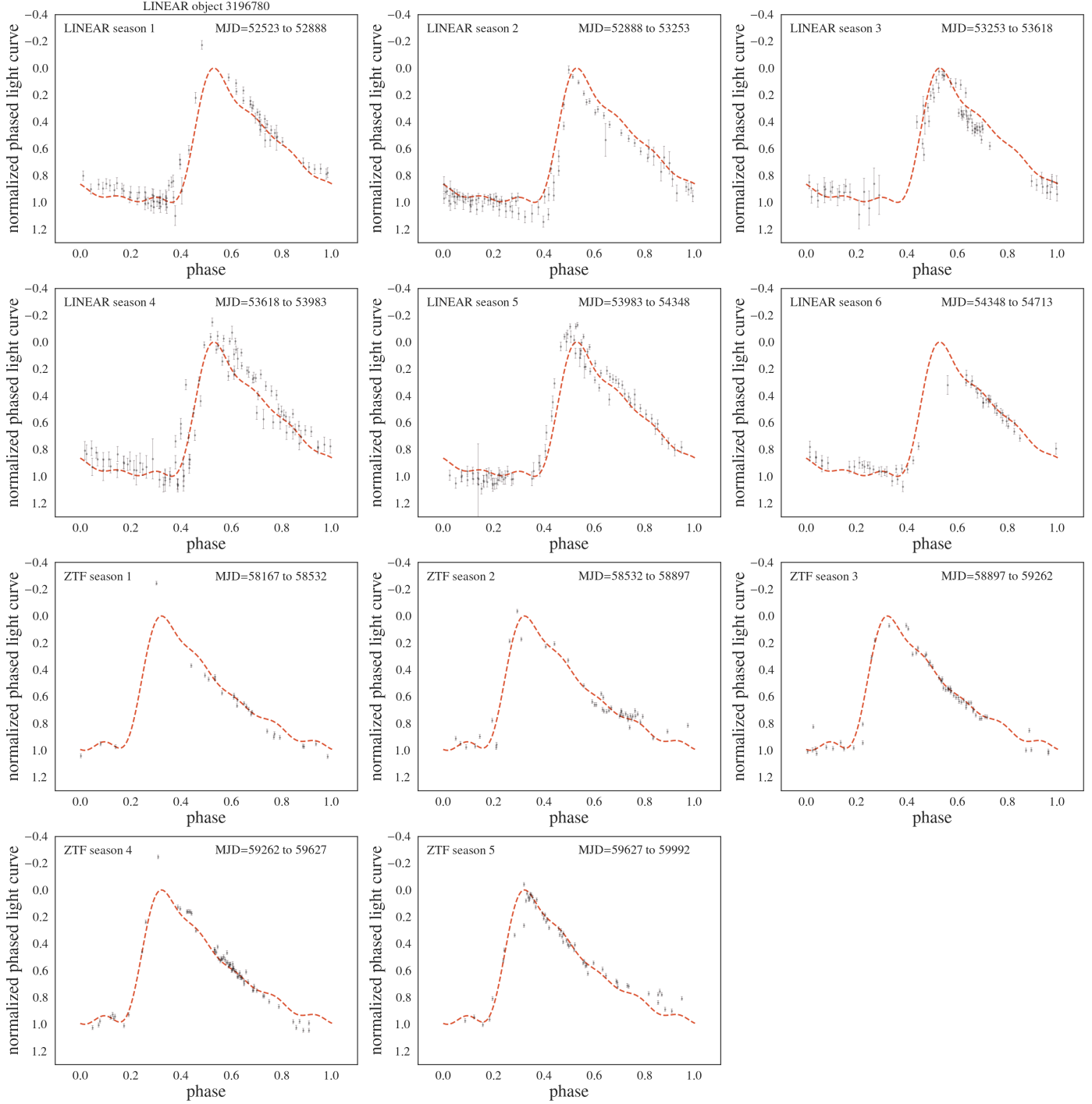


Fig. 12. Analogous to Fig. 8, except that star with LINEARid = 3196780 is shown. Amplitude modulation is clearly seen in LINEAR light curves (top two rows), while not discernible in ZTF light curves (bottom two rows). Additional stars with similar behavior include LINEARid = 2889542, 7723614, 8342007. This behavior strongly suggests that Blazhko effect can appear and disappear on time scales shorter than about a decade.

Appendix A: Full table of results

464
465
466
467
468

The first 50 confirmed Blazhko stars with their LINEAR IDs in the first column and then, for both LINEAR and ZTF, their computed light curve periods, the number of data points per light curve, robust and ordinary χ^2 values, and light curve amplitudes, followed by amplitude difference between LINEAR and ZTF, the strength and period of Blazhko peaks in their periodograms, light curve type (1: ab, 2: c), detection significance flag for the periodograms (Z, L or “-” for no detection; the strength and period of Blazhko peaks are not reliable when “-”) and the selection score (see Sections 3.1 and 3.2 for details). The full table is available in online edition.

LINEAR ID	Plinear	Pztf	N_L	N_Z	L_chi2r	Z_chi2r	L_chi2	Z_chi2	Lampl	Zampl	Ampl_dif	BpeakL	BpeakZ	BperiodL	BperiodZ	LCtype	Periodogram_f	B_score
158779	0.609207	0.609189	293	616	1.6	3.9	3.7	34.2	0.47	0.68	0.21	1.6443	1.6444	352.7337	350.2627	1	-	7
263541	0.558218	0.558221	270	503	2.9	6.6	15.8	110.4	0.64	0.82	0.18	1.8621	1.8025	14.1513	89.9685	1	-	7
393084	0.530027	0.530033	493	372	1.1	3.2	1.6	19.2	0.96	1.31	0.35	1.9447	1.8896	17.2369	347.2222	1	-	6
810169	0.465185	0.465212	289	743	2.1	2.8	6.0	15.1	0.77	0.75	0.02	2.2232	2.2230	13.6017	13.6082	1	-	5
924301	0.507503	0.507440	418	189	1.9	9.3	13.8	162.9	0.87	0.79	0.08	2.0043	1.9763	29.5072	178.4121	1	-	8
970326	0.592233	0.592231	275	552	1.1	2.1	1.9	7.7	0.51	0.75	0.24	1.7563	1.6992	14.7656	93.2836	1	-	5
999528	0.658401	0.658407	564	213	1.2	2.7	1.8	21.7	0.57	0.92	0.35	1.5527	1.5510	29.5247	31.0366	1	-	5
1005497	0.653607	0.653605	607	192	1.1	2.1	2.1	12.4	0.60	0.83	0.23	1.5639	1.5481	29.4638	55.1116	1	-	5
1092244	0.649496	0.649558	590	326	1.2	3.6	2.3	32.1	0.72	0.58	0.14	1.5735	1.5640	29.5421	40.8330	1	-	7
1240665	0.632528	0.632522	468	311	3.0	1.1	25.2	1.6	0.33	0.33	0.00	1.6149	1.5865	29.4942	182.3154	1	Z	0
1244554	0.536875	0.536962	469	312	1.8	2.3	9.5	14.8	0.71	0.97	0.26	1.8966	1.9325	29.4638	14.2481	1	-	7
1271119	0.565270	0.565257	280	521	1.0	4.0	2.9	45.5	0.69	0.90	0.21	1.8366	1.7739	14.8060	208.3333	1	-	6
1332201	0.580711	0.580731	260	208	1.6	4.2	9.2	50.1	0.59	0.83	0.24	1.7559	1.7918	29.4942	14.3225	1	-	7
1390653	0.521867	0.521871	524	310	1.3	4.1	4.2	44.9	1.10	1.28	0.18	1.9502	2.0026	29.4291	11.5768	1	-	6
1448299	0.606912	0.606940	435	267	2.7	5.4	32.5	35.6	0.77	0.70	0.07	1.6816	1.6531	29.4551	180.9955	1	-	8
1539000	0.500288	0.500279	410	468	1.5	3.6	6.1	66.3	0.89	1.13	0.24	2.0021	2.0017	303.9514	355.8719	1	-	6
1593736	0.592628	0.592650	264	532	1.2	5.7	2.1	35.9	0.37	0.36	0.01	1.7584	1.6910	14.0795	272.4796	1	-	6
1748058	0.310237	0.310176	463	272	1.4	5.7	2.2	30.7	0.38	0.23	0.15	3.2572	3.2297	29.5203	173.3102	2	-	7
1790596	0.534498	0.534506	509	327	3.1	3.3	19.3	15.6	0.79	0.70	0.09	1.9046	1.8764	29.6868	182.1494	1	-	6
1882354	0.695061	0.695029	313	411	1.5	2.8	3.0	13.2	0.63	0.70	0.07	1.4909	1.4419	19.1516	326.2643	1	-	6
1936459	0.649248	0.649240	431	268	0.7	1.1	0.6	1.7	0.45	0.43	0.02	1.5741	1.5458	29.5203	181.8182	1	Z	0
2041979	0.653694	0.653639	276	1378	1.2	5.3	1.5	57.5	0.63	0.64	0.01	1.5944	1.5816	15.4607	19.3442	1	-	7
2050107	0.686454	0.686466	190	1388	3.9	3.3	16.4	22.3	0.78	0.64	0.14	1.4906	1.4633	29.5159	151.2859	1	-	6
2122319	0.359422	0.359424	519	199	2.1	6.1	7.2	36.6	0.38	0.55	0.17	2.8161	2.8926	29.5421	9.0645	2	-	7
2229607	0.575179	0.575211	290	731	1.2	4.4	2.7	38.3	0.55	0.81	0.26	1.8093	1.7433	14.1383	207.2539	1	-	8
2243683	0.579777	0.579803	531	262	3.1	4.3	22.0	36.0	0.52	0.56	0.04	1.7588	1.7303	29.4204	180.0180	1	-	6
2264042	0.655373	0.655391	391	299	1.6	4.0	6.5	57.4	0.74	0.76	0.02	1.5597	1.5313	29.5465	182.4818	1	-	5
2280940	0.562372	0.562374	310	735	1.1	3.2	1.4	17.5	0.84	1.01	0.17	1.8461	1.7847	14.7286	153.2567	1	-	6
2333087	0.5511462	0.5511424	560	202	3.5	8.0	29.8	90.2	0.72	0.88	0.16	1.8473	1.8304	29.5072	59.0842	1	-	9
2334384	0.555341	0.555333	443	204	2.0	6.5	10.5	84.7	0.63	0.88	0.25	1.8346	1.8353	29.5377	28.9394	1	-	7
2397296	0.488814	0.488836	522	196	1.2	6.6	3.2	78.9	0.65	1.01	0.36	2.0796	2.0672	29.5421	46.5224	1	-	9
2414841	0.559611	0.559592	522	305	1.7	5.7	5.6	62.8	0.69	1.09	0.40	1.8208	1.7920	29.5421	201.2072	1	-	8
2612592	0.5711562	0.5711543	270	1391	1.3	2.8	2.4	24.8	0.76	0.70	0.06	1.8173	1.7544	14.7787	208.5506	1	-	5
2683009	0.606278	0.606210	180	892	6.6	7.4	63.6	88.8	0.82	0.52	0.30	1.6833	1.6603	29.4942	93.7207	1	-	9
2851826	0.521838	0.521842	257	653	1.0	2.5	1.6	18.1	0.95	1.21	0.26	1.9595	1.9595	23.1642	23.1374	1	-	5
2889542	0.570913	0.570911	457	170	1.3	2.5	2.7	9.2	0.96	1.35	0.39	1.7855	1.8062	29.4855	18.3268	1	-	5
2892940	0.539855	0.539896	462	169	1.3	4.2	3.7	49.1	0.90	1.21	0.31	1.8862	1.9288	29.5290	13.0514	1	-	8
2936953	0.328746	0.328733	271	187	2.7	1.3	13.0	2.5	0.35	0.29	0.06	3.1123	3.0448	14.1995	356.5062	2	-	5
3140139	0.304590	0.304585	255	343	2.5	5.6	7.7	25.1	0.40	0.60	0.20	3.3529	3.4219	14.3338	7.2056	2	-	7
3183285	0.349653	0.349664	485	588	1.2	2.8	4.1	15.7	0.48	0.58	0.10	2.8939	2.8654	29.4768	181.8182	2	-	5
3196582	0.268017	0.268018	479	172	2.5	3.4	8.6	10.1	0.35	0.51	0.16	3.7650	3.8361	29.5203	9.5256	2	-	6
3196780	0.504148	0.504199	475	286	2.2	3.2	9.3	21.5	0.81	0.85	0.04	2.0029	1.9889	51.7331	181.6530	1	-	6
3219035	0.326746	0.326509	376	168	3.9	2.6	23.9	11.5	0.32	0.23	0.09	3.1287	3.0661	14.6692	294.1176	2	-	7
3463199	0.334718	0.334710	297	579	0.7	2.3	0.6	11.3	0.51	0.67	0.16	3.0584	2.9952	14.1153	133.2445	2	-	5
3491287	0.490986	0.490995	483	504	1.4	3.8	4.1	37.9	0.94	0.80	0.14	2.0537	2.0537	58.8408	58.8755	1	-	5
3589854	0.612893	0.612953	468	545	3.9	5.8	29.1	45.0	0.49	0.50	0.01	1.6656	1.6369	29.4031	184.6722	1	-	7

470